Maximal Migration of Human Smooth Muscle Cells on Fibronectin and Type IV Collagen Occurs at an Intermediate Attachment Strength

Paul A. DiMilla, Julie A. Stone, John A. Quinn, Steven M. Albelda,* and Douglas A. Lauffenburger‡

Departments of Chemical Engineering and *Medicine, University of Pennsylvania, Philadelphia, Pennsylvania 19104; and ‡Departments of Cell and Structural Biology and Chemical Engineering, University of Illinois at Urbana-Champaign, Urbana, Illinois 61801

Abstract. Although a biphasic dependence of cell migration speed on cell–substratum adhesiveness has been predicted theoretically, experimental data directly demonstrating a relationship between these two phenomena have been lacking. To determine whether an optimal strength of cell–substratum adhesive interactions exists for cell migration, we measured quantitatively both the initial attachment strength and migration speed of human smooth muscle cells (HSMCs) on a range of surface concentrations of fibronectin (Fn) and type IV collagen (CnIV). Initial attachment strength was measured in order to characterize short time-scale cell-substratum interactions, which may be representative of dynamic interactions involved in cell migration.

The critical fluid shear stress for cell detachment, determined in a radial-flow detachment assay, increased linearly with the surface concentrations of adsorbed Fn and CnIV. The detachment stress required for cells on Fn, $3.6 \pm 0.2 \times 10^{-3}$ μdynes/absorbed molecule, was much greater than that on CnIV, $5.0 \pm 1.4 \times 10^{-5}$ μdynes/absorbed molecule. Time-lapse videomicroscopy of individual cell movement paths showed that the migration behavior of HSMCs on these substrates varied with the absorbed concentration of each matrix protein, exhibiting biphasic dependence. Cell speed reached a maximum at intermediate concentrations of both proteins, with optimal concentrations for migration at 1×10^3 molecules/μm² and 1×10^4 molecules/μm² on Fn and CnIV, respectively. These optimal protein concentrations represent optimal initial attachment strengths corresponding to detachment shear stresses of 3.8 μdyne/μm² on Fn and 1.5 μdyne/μm² on CnIV. Thus, while the optimal absorbed protein concentrations for migration on Fn and CnIV differed by an order of magnitude, the optimal initial attachment strengths for migration on these two proteins were very similar. Further, the same minimum strength of initial attachment, corresponding to a detachment shear stress of ~1 μdyne/μm², was required for movement on either protein.

These results suggest that initial cell–substratum attachment strength is a central variable governing cell migration speed, able to correlate observations of motility on substrata differing in adhesiveness. They also demonstrate that migration speed depends in biphasic manner on attachment strength, with maximal migration at an intermediate level of cell–substratum adhesiveness.

MIGRATION of tissue cells and white blood cells plays a critical role in a diverse array of physiological and pathological phenomena, including the proper development and repair of organs, inflammation, angiogenesis, and metastasis (Trinkaus, 1984). Important features of cell migration have been outlined previously (e.g., Lackie, 1986; Singer and Kupfer, 1986; Devreotes and Zigmond, 1988; Heath and Holifield, 1991). Three general characteristics have been identified for persistent cell locomotion over adhesive substrata: (*a*) cytoskeletal elements generate intracellular mechanical stresses; (*b*) cell–substratum traction created by dynamic adhesion processes transform these stresses into a displacement force on the cell body; and (*c*) morphological polarization channels this force unidirectionally as required for cell body translocation. In this paper we investigate the second characteristic, the effect of cell–substratum adhesive interactions on migration speed.

Dynamic cell–substratum adhesion processes during migration are mediated in many cells by specific reversible interactions between transmembrane glycoproteins known as integrins (Hynes, 1987; Yamada, 1989; Albelda and Buck, 1990; Hemler, 1990) and substratum-bound extracellular matrix (ECM)[1] proteins (Straus et al., 1989; Bauer et al.,

Dr. DiMilla's present address is Department of Chemical Engineering, Carnegie Mellon University, Pittsburgh, PA 15213.

1. *Abbreviations used in this paper*: CnIV, type IV collagen; ECM, extracellular matrix; Fn, fibronectin; HSCM, human smooth muscle cell; RFDA, radial-flow detachment assay.

1992). Because integrins bind both ECM proteins and cytoskeletal elements with low affinity, $K_d \sim 10^{-6}$ M for both integrin–Fn (Akiyama and Yamada, 1985) and integrin–talin interactions (Horwitz et al., 1986), they are attractive candidates for the role of translating intracellular stresses to extracellular traction (Burridge et al., 1988).

Cell migration as well as morphology may depend on the strength of transient cell–substratum attachments (Stein and Bronner, 1989), and three regions of motile and morphological behavior can be envisioned for a cell interacting with a surface. On weakly adhesive surfaces cell–substratum interactions cannot provide traction, so that no locomotion is possible and the cell spreads poorly. On strongly adhesive surfaces the cell is well-spread and immobilized, so regular dynamic disruption of cell–substratum attachments is difficult and locomotion again does not occur. For an intermediate strength of cell–substratum interactions, however, cell body translocation may be possible. The terms weak and strong adhesion are relative to the level of motile force generated within the cell and transmitted to the cell–substratum attachments. Detailed predictions have been generated using a mathematical model based on this concept (DiMilla et al., 1991). Model computations indicate that a key variable governing cell migration speed is the ratio of intracellular motile force to cell–substratum attachment strength, and that migration speed should exhibit a biphasic dependence on the attachment strength for a given level of motile force.

Several recent studies have demonstrated that variations in either the adsorbed concentration of substratum-bound ligands for integrins or integrin–ligand affinity can affect motility. Goodman et al. (1989) found a biphasic relationship between the movement of murine skeletal myoblasts and the adsorbed concentration of either laminin or the cell-binding laminin fragment E8. Duband et al. (1991) also observed that the extent of migration for neural crest cells decreased with increasing surface concentration of high-affinity antibodies against the β_1 subunit but was enhanced by increasing concentrations of corresponding low-affinity antibodies. However, the prediction that an optimal strength of cell–substratum adhesion exists for maximal cell migration speed has not yet been directly tested. Determination of whether an optimal ligand concentration and an optimal strength of attachment for migration are equivalent requires application of an adhesion assay in which the strength of cell–substratum attachment is measured quantitatively. Most previous studies of attachment have focused on either qualitative observations of cell morphology or measurement of the fraction of cells that resist detachment in a standard manual washing assay. These approaches typically do not provide quantitative measures of cell–substratum attachment strength.

In this work we examine the relationship between the strength of initial cell–substratum attachment and the rate of migration of individual human adult vascular smooth muscle cells (HSMCs) on surfaces coated with the ECM proteins fibronectin (Fn) and type IV collagen (CnIV). Alterations in the motile properties of these cells have been implicated in the development of atherosclerotic plaques (Ross, 1986) and in deleterious vascular remodeling after injury (Clyman et al., 1990). HSMCs express on their surface integrins which can bind to Fn and CnIV (S. Albelda, unpublished observations). We focus on initial attachment strength in order to characterize short time-scale cell–substratum interactions, which we believe may be relevant to dynamic interactions involved in cell migration. For tissue cells exhibiting typical locomotion rates on the order of 10–20 μm/h, attachments must be dynamic on the time scale of a few hours or less. Regen and Horwitz (1992) recently have shown that locomotion involves dissociation of adhesion receptor–ECM linkages as well as distraction of adhesion receptors from the cell membrane.

Using a novel radial-flow detachment assay (Cozens-Roberts et al., 1990; DiMilla et al., 1992*a*) and an assay for individual cell migration consisting of time-lapse videomicroscopy, image analysis, and application of a persistent random walk model (DiMilla et al., 1992*b*), we determine quantitatively the dependence of both the fluid shear stress required for detachment of HSMCs and the movement speed of HSMCs on the adsorbed concentration of Fn and CnIV. We show that HSMC migration on both Fn and CnIV requires the same strength of initial attachment, and that the migration speeds on both are maximal at intermediate attachment strengths of similar magnitudes. These results are consistent with the model predictions of DiMilla et al. (1991) that migration speed should exhibit a biphasic dependence of migration on short time scale adhesiveness. Migration speeds on the two proteins are correlated more satisfactorily by reference to attachment strength than to absorbed protein concentration, indicating that the strength of initial cell–substratum adhesive interactions is the more central variable.

Materials and Methods

Cell Culture

HSMCs isolated from segments of iliac arteries from renal donors were grown as previously described (Tan et al., 1991; DiMilla et al., 1992*b*). Cells were maintained in gelatinized flasks in complete medium consisting of medium 199 (GIBCO BRL, Gaithersburg, MD), 10% heat-inactivated FBS (GIBCO BRL), 74 μg/ml endothelial cell growth factor, 100 μg/ml heparin, and 2 mM glutamine. For experiments, cells between cumulative population doublings 15 and 20 were removed with 0.25% trypsin/versine (GIBCO BRL), treated with 0.2 wt% soybean trypsin inhibitor (Worthington Biochemical, Freehold, NJ) in serum-free MCDB-104 medium (formula No. 82-5006EA; GIBCO BRL) supplemented with 25 mM Hepes (Sigma Immunochemicals, St. Louis, MO) and 10 μg/ml gentamicin antibiotic (Sigma Immunochemicals), spun at 1,500 rpm for 10 min, and resuspended in supplemented MCDB-104 medium. HSMCs cultured in serum-free MCDB-104 medium (developed to support clonal cell growth) maintained normal morphology and viability for up to 3 d, in contrast to a rapid deterioration of cells in serum-free medium 199 or DME.

Preparation and Characterization of Fn and CnIV Substrata

ECM proteins were prepared as described previously (DiMilla et al., 1992*c*). A sterile stock solution of human plasma Fn (Boehringer Mannheim Biochemicals, Indianapolis, IN) was prepared by thawing lyophilized 1-mg or 100-μg aliquots in sterile PBS. 1 mg/ml CnIV in 1 mM acetic acid (a gift of Dr. Stuart Williams, Thomas Jefferson University, Philadelphia, PA) was diluted into 0.01 M $NaHCO_3$ to form a stock solution at 100 μg/ml. All protein solutions were stored at 4°C and serially diluted in PBS as needed.

For attachment and migration assays 60- and 35-mm-diam bacteriological polystyrene dishes (Falcon Nos. 1007 and 1008; Becton Dickinson Labware, Lincoln Park, NJ) were coated with 4.4 and 1.5 ml solutions of ECM protein, respectively, at known soluble concentrations for 24 h at 4°C. These volumes exposed both substrata to the same number of protein molecules per area at a given soluble concentration. Unbound ECM protein was aspirated and an equivalent volume of sterile 1 wt% heat-denatured BSA (Fraction V; 96–99% albumin, Sigma Immunochemicals) was added to

Table I. Relationships between Soluble and Adsorbed Surface Concentrations of Fn and CnIV

Substrate	Concentration		Cells Tracked	
	Coating	Adsorbed	Total	Motile
	($\mu g/ml$)	($molecules/\mu m^2$)		
Fn	3.5	3.2×10^2	64	10
Fn	5.0	4.6×10^2	–	–
Fn	10.0	8.0×10^2	66	25
Fn	22.9	1.0×10^3	76	45
Fn	25.0	1.1×10^3	–	–
Fn	50.0	1.6×10^3	64	12
Fn	100.0	2.6×10^3	74	11
CnIV	1.0	3.0×10^2	28	2
CnIV	7.0	3.0×10^3	56	14
CnIV	13.3	7.0×10^3	53	32
CnIV	15.0	8.1×10^3	–	–
CnIV	20.0	1.1×10^4	62	48
CnIV	25.0	1.4×10^4	–	–
CnIV	41.3	2.6×10^4	59	50
CnIV	50.0	3.2×10^4	–	–
CnIV	62.0	4.0×10^4	70	43

Non-tissue culture dishes were coated with indicated soluble concentrations of Fn or CnIV, nonspecific adhesion blocked with BSA, and dishes washed 3× with PBS before cells added. Adsorbed surface concentrations of ECM protein were determined from a companion study of protein adsorption as reported in DiMilla et al. (1992*c*). The total number of spread and isolated cells tracked and the subset of this population which were motile in assays for individual cell migration are listed. All techniques are described in detail in Materials and Methods.

each surface for 45 min at room temperature to block nonspecific interactions. The BSA solution was aspirated and each surface washed three times with sterile PBS. We determined the absorbed surface concentration of Fn and CnIV corresponding to each soluble concentration (Table I) from direct measurements of the amount of ^{125}I-labeled ECM protein on bacteriological dishes prepared following the procedures described here (DiMilla et al., 1992*c*).

Assay for Initial Cell–Substratum Attachment Strength

Cell–substratum attachment was measured using a modified radial-flow detachment assay (RFDA) (DiMilla et al., 1992*a*), based on the RFDA originally developed by Cozens-Roberts et al. (1990). In our assay HSMCs adhering to a 60 mm-diameter disk were exposed to an axisymmetric fluid shear flow in which the hydrodynamic shear stress on the cells, s (in μdynes/μm^2), decreases with the radial distance, r (in mm), from a central inlet point

$$s = \frac{1.5\ Q^*}{r - 1.7} \tag{1}$$

where Q* is the effective volumetric flow rate (in ml/s). During detachment under flow adherent HSMCs were removed from the inner region of the disk, where fluid shear forces exceeded the adhesive forces between the cells and the underlying surface, but remained attached in the outer region, where the fluid velocity and shear forces were smaller. The radial position at which 50% of the cells detached at equilibrium was defined by convention as the critical radius, r_c (Cozens-Roberts et al., 1990). The critical shear stress for detachment, s_c, representing a quantitative measure of the force necessary to detach cells, was defined as the result of Eq. 1 with $r = r_c$.

Operation of a RFDA to measure cell attachment has been described previously (DiMilla et al., 1992*a*). All procedures were conducted at room temperature. $1.0 - 2.5 \times 10^5$ cells in 1 ml supplemented MCDB-104 medium were added to a 60-mm-diam dish coated with ECM protein and BSA. A cylindrical plexiglass probe then was inserted carefully into the dish and secured in place with an overlying collar to form an assembled flow chamber. After 30 min a constant flow of supplemented MCDB-104 was established by gravity feed from a constant head tank and maintained for 10 to 20 min to establish a stable pattern of detachment. In some experiments Dextran T500 (Pharmacia Fine Chemicals, Piscataway, NJ) was added to the flow medium to increase viscosity and generate higher shear stresses under conditions of laminar flow (adding 1.7% Dextran T500 approximately doubled the viscosity). Flow was stopped and the flow chamber carefully disassembled so that the remaining adherent cells were not disturbed. The cells were fixed and stained with 95% ethanol (Pharmacia Fine Chemicals) in water for 10 min and 2% crystal violet (Sigma Immunochemicals) in PBS. Critical radii were measured using a stereo microscope (Carl Zeiss, Thornwood, NY) as the average of quadruplicate readings of x-y stage displacement, and s_c calculated.

The relationship between critical shear stress for detachment and adsorbed concentration of Fn and CnIV was assessed using a linear regression analysis applied to means and SDs for the s_c measured at each concentration of ECM protein. Values for linear regression parameters for Fn and CnIV were compared using an F test (Mendenhall and Sincich, 1992).

Assay for Individual Cell Migration Properties

Observations of Cell Morphology. $0.9 - 1.8 \times 10^4$ HSMCs in 2 ml of supplemented MCDB-104 medium were added to a 35-mm-diam dish coated with ECM protein and BSA. The dish was sealed with parafilm and cells allowed to spread overnight at 37°C. Cells were observed at 10× magnification under phase-contrast optics using a Zeiss Axiovert 10 inverted microscope and a Hamamatsu C2400 videocamera (Photonic Microscopy, Oak Brook, IL). The morphology of HSMCs depended on the concentration of adsorbed Fn. At low concentration of 3.2×10^2 molecules/μm^2 cells were poorly spread and unpolarized in appearance. However, as the concentration of Fn was increased to 1.0×10^3 molecules/μm^2, cells became bipolar with lengths on the order of 50–100 μm. Further increases in the concentration of Fn to 2.6×10^3 molecules/μm^2 resulted in cells that not only were elongated but also spread laterally. We observed similar trends with respect to increasing concentration for HSMCs on CnIV. However, the concentration of CnIV had to be increased over two orders of magnitude (from 3.0×10^2 to 4.0×10^4 molecules/μm^2) to produce the same range of changes in morphology achieved by a one order of magnitude increase in the surface concentration of Fn, although similar ranges of coating concentrations were used. In contrast, HSMCs did not attach and spread on the surface of control dishes coated only with BSA.

Time-lapse Videomicroscopy and Image Analysis. Time-lapse videomicroscopy and image analysis were conducted as previously described (DiMilla et al., 1992*b*). 30 fields on the dish were selected with a joystick and scanned sequentially once every 15 min using a Mertzhauser IM-EK32 motorized stage (Opto-Systems, Newtown, PA) and MAC 1000 controller (Ludl Electronic Products, Hawthorne, NY). Cell behavior over 48 h was recorded continuously at 1/120 of real time with a time-lapse VCR (model BR-9000U; JVC, Elmwood Park, NJ). Temperature on the stage was maintained at 37°C using an ASI 400 Air Stream Incubator (Nicholson Precision Instruments, Gaithersburg, MD).

Movement of individual HSMCs was followed by playback of videos through an image processing system consisting of a FA-400 time-base corrector (FOR-A Corporation of America, Boston, MA), a series 151 image processor (Imaging Technology, Woburn, MA), and a PC-AT 286 microcomputer (AST Research, Irvine, CA). We applied this system to track the position of centroids of individual cells at intervals of $\Delta t = 15$ min for up to 36 h using a semiautomated algorithm in which a single field was analyzed at a time (DiMilla et al., 1992*b*). Only isolated and spread cells were tracked. For each cell tracked a series of pixel coordinates as a function of elapsed tracking time, $n\Delta t$, was determined. These coordinates were converted to real physical displacements and could be plotted to provide a qualitative description of the path traveled by each individual cell. "Windrose" displays (Goodman et al., 1989) illustrating the qualitative motile behavior of ten typical cells on a substrata were produced by linking centroid positions at intervals of 30 min and superimposing the starting position of each cell to a common origin.

Measurement of Cell Migration Parameters. In uniform extracellular environments isolated HSMCs move as persistent random walkers: the mean-squared displacement, $\langle d^2 \rangle$, of each motile cell is a function of time, t, speed, S, and persistence time, P (DiMilla et al., 1992*b*):

$$\langle d^2 \rangle = 2S^2P\left[t - P\left(1 - e^{-\frac{t}{P}}\right)\right]. \tag{2}$$

While the parameter S can be interpreted as simply the "rate" at which a cell moves, the parameter P represents a measure of the average time period between "significant" changes in the direction of movement. For a cell tracked a total of $t_{max} = N\Delta t$ min with the series of real spatial coor-

dinates, $\{x(n\Delta t), y(n\Delta t)\}$, we calculated mean-squared displacements as a function of time interval $t = n\Delta t$ as

$$\langle d^2(t = n\Delta t)\rangle = \frac{1}{(N - n + 1)} \sum_{i=0}^{N-n} [[x((n + i)\Delta t) - x(i\Delta t)]^2 + [y((n + i)\Delta t) - y(i\Delta t)]^2]. \quad (3)$$

Values of S and P for each motile cell were determined by fitting Eq. 2 to experimental data from Eq. 3. Immotile cells, distinguished by negligible displacements relative to their body length over long observation times and small persistence times relative to Δt, were assigned a speed of 0 μm/hr and persistence time undefined (the concept of persistence time was not applicable for these latter cells) (DiMilla et al., 1992*b*). Values of S and P for cells tracked <6 h or with $P > t_{max}/3$ were excluded from further analysis because these cells had not been observed long enough to identify the true tortuosity of their paths (Stokes et al., 1991). The percentage of cells that were motile, %-motile cells, was also determined as previously described (DiMilla et al., 1992*b*).

For each ECM substrate, means and standard errors for speed were calculated based on best-fit values for all cells (motile and immotile) observed on that substrate, while the corresponding statistics for persistence time could be calculated only for motile cells. Previous studies of HSMC migration have shown that speed follows a normal distribution truncated at zero speed whereas persistence time follows an exponential distribution (DiMilla et al., 1992*b*). Standard deviations for %-motile cells were estimated by assuming that a binomial distribution described the observation of a motile cell. Differences among means were compared using Tukey's method for multiple comparisons as an analysis of variance (Mendenhall and Sincich, 1992).

Results

To address whether the adhesion and motility behaviors of HSMCs depend on the concentration of Fn and CnIV molecules on the underlying substratum, we coated non-tissue culture petri dishes with various concentrations of Fn or CnIV overnight at 4°C. We subsequently exposed these surfaces to 1% BSA for 45 min to block nonspecific adhesion (Basson et al., 1990). We present our data for attachment and migration as a function of surface concentration because we previously have determined the relationship between the soluble concentration of Fn or CnIV used to coat a surface and the actual adsorbed concentration of these molecules (DiMilla et al., 1992*c*). Identical surfaces, proteins, and procedures for coating were used in this companion study and the experiments described here.

Strength of HSMC–Substratum Attachment Depends on Concentration of Fn and CnIV

To examine the attachment of HSMCs after incubation for 30 min to surfaces coated with increasing concentrations of ECM protein, we applied a radial-flow detachment assay (RFDA) in which the strength of cell–substratum attachment was measured quantitatively as the critical fluid shear stress for detachment, s_c (DiMilla et al., 1992*a*). Based on measurements of the critical radius for detachment, r_c—the radial distance from the center of the dish (across from the fluid inlet) at which hydrodynamic detachment and cell–substratum adhesive forces balanced—and Eq. 1, we determined the relationship between s_c and the concentration of ECM protein for HSMCs after incubation for 30 min on these surfaces (Fig. 1). The critical shear stress increased monotonically with the adsorbed surface concentration of Fn and CnIV: greater fluid forces were required to detach HSMCs from surfaces coated with greater concentrations of ECM protein. For both ECM proteins the relationship between

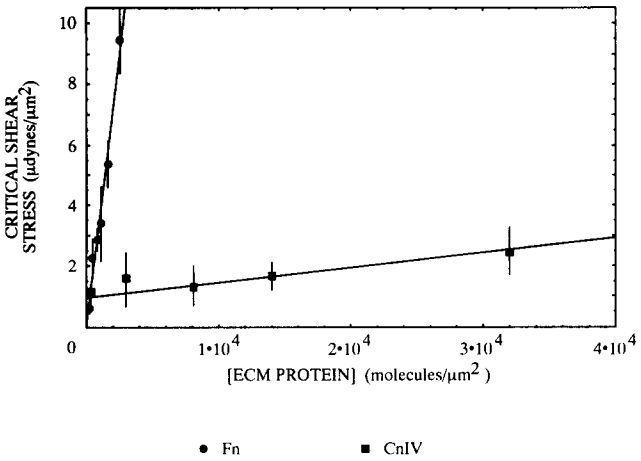

Figure 1. Effect of surface concentration of adsorbed Fn and CnIV on the strength of cell–substratum attachment of HSMCs as measured in a radial flow detachment assay. The critical shear stress for cell detachment, s_c, was calculated using Eq. 1, after a 30-min incubation on protein-coated bacteriological polystyrene dishes at room temperature. Data for Fn (•) and CnIV (■) are means and standard errors from three to four dishes at each protein concentration. Surface protein concentrations were determined from a companion study of protein adsorption as reported in DiMilla et al. (1992*c*), summarized in Table I. Lines represent linear least-squares fits of data with slopes of $3.6 \pm 0.2 \times 10^{-3}$ μdynes/Fn molecule and $5.0 \pm 1.4 \times 10^{-5}$ μdynes/CnIV molecule.

critical shear stress and surface concentration was linear, even though the surface concentrations of CnIV were much greater than those of Fn; roughly an order of magnitude more CnIV than Fn adsorbed at a given coating concentration (DiMilla et al., 1992*c*). Based on a linear least-squares analysis, s_c increased by $3.6 \pm 0.2 \times 10^{-9}$ dynes/adsorbed Fn molecule and $5.0 \pm 1.4 \times 10^{-11}$ dynes/adsorbed CnIV molecule (values are means ± SDs). The difference between these slopes was statistically significant (based on a regression analysis with a 95% confidence level from an F test). This difference, directly reflected in the larger range of shear forces required for detachment on Fn compared to CnIV, demonstrates that HSMCs adhered approximately 70 times more tightly per Fn molecule than per CnIV molecule on these surfaces.

Migration Paths of Individual HSMCs Depend on Concentration of Fn and CnIV

To determine how the adsorbed concentrations of ECM protein affect motility, we examined the migration of individual HSMCs on non-tissue culture dishes coated with Fn or CnIV and blocked with BSA, following the procedures used for the RFDA. To allow isolated cells to move for a period of hours to days without encountering each other, HSMCs were plated at sparse concentrations of 1–2 10^3 cells/cm^2. With our time-lapse videomicroscopy system we observed that cell movement over a time scale of minutes on surfaces with moderate and high concentration of ECM protein appeared to follow a saltatory cycle of lamellipodal extension and uropodal retraction, consistent with previous observations of crawling fibroblasts (e.g., Trinkaus, 1984). During lamellipodal extension the body of the cell remained relatively stationary, while retraction of the tail was more abrupt than lamellipodal progression and occasionally resulted in the

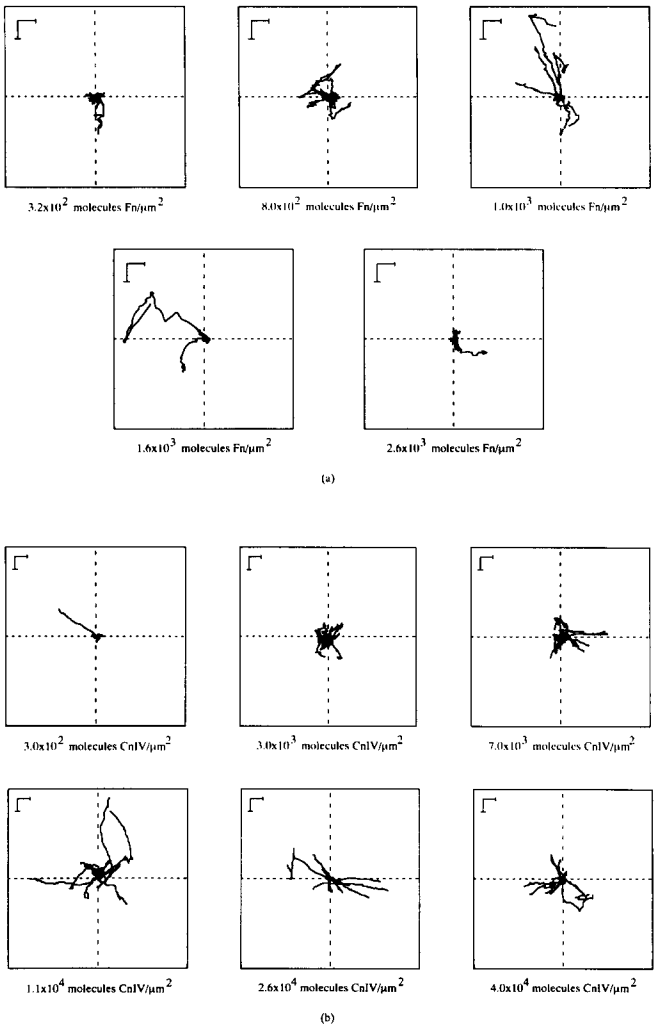

Figure 2. Typical cell paths over 24 h for HSMCs migrating at 37°C on increasing concentrations of (*a*) FN and (*b*) CnIV. Motile behavior of isolated HSMCs in serum-free MCDB-104 medium was recorded using time-lapse videomicroscopy for cells on bacteriological polystyrene dishes coated with Fn or CnIV and BSA. Continuous paths of centroid position for 10 typical cells on each ECM protein concentration, determined by tracking cells at 30-min intervals with an image processor, were superimposed to a common origin in wind-rose displays. All techniques are described in detail in Materials and Methods. Surface concentrations of Fn and CnIV for each individual wind-rose plot are indicated (Table I). Bars, 100 μm.

deposition of uropodal fragments, especially for rapidly moving cells on substrata with higher concentrations of CnIV or Fn.

We identified qualitative differences in motile behavior resulting from variations in the adsorbed concentration of ECM protein by applying time-lapse videomicroscopy and image analysis to track the paths traveled by individual HSMCs. Typical paths over 24 h for 10 isolated cells on various concentrations of Fn and CnIV are presented in Fig. 2, *a* and *b*, respectively, as "wind-rose" displays in which the starting position of each cell is superimposed to a common origin (Goodman et al., 1989). The ranges of absorbed concentrations examined here and with the RFDA are similar; corresponding soluble coating concentrations are given in Table I. On a low concentration of 3.2×10^2 molecules Fn/μm^2, few cells moved significantly, but increasing the surface concentration of Fn by factors of approximately two and three progressively caused most cells to migrate hundreds of microns over the period of 24 h (Fig. 2 *a*). No single direction of movement was preferred, consistent with random motility in the absence of biasing gradients. Further increases in the absorbed Fn concentration to 1.6×10^3 and 2.6×10^3 molecules/μm^2 progressively decreased the extent of movement of individual cells.

We observed similar trends for isolated HSMCs on CnIV (Fig. 2 *b*), although the extent of movement was not diminished as significantly at high absorbed protein concentrations as it was for Fn. This result is likely due to the relative inability to produce highly adhesive surfaces even at high concentrations of adsorbed CnIV, as seen in Fig. 1. We did not examine the behavior of HSMCs on concentrations of CnIV $>4 \times 10^4$ molecules/μm^2 because these concentrations would significantly exceed expectations for a close-packed monolayer, and the actual concentration of protein exposed at the surface would be ill defined.

These trends for migration behavior were in parallel with trends observed for cell morphology (see Materials and Methods), for which cells were poorly spread and unpolarized at low absorbed ECM protein concentrations, became bipolar at intermediate concentrations, and were found to be spread laterally at high concentrations.

Quantitative Motility Parameters for HSMCs Depend on Concentration of Fn and CnIV

Although comparison of typical cell paths revealed qualitative differences in the motile behavior of HSMCs on different substrates, the parameters %-motile cells, speed (S), and persistence time (P) are more rigorous quantitative measures of how the intrinsic motility of these cells varies with the surface concentrations of Fn and CnIV. We determined these parameters from individual cell paths by modeling cell movement as a persistent random walk (Gail and Boone, 1970). It has been demonstrated that this approach distinguishes motile characteristics more properly than do other common methods, such as calculating the average distance migrated in an arbitrary time interval (Dunn, 1983). Our results are derived from analysis of the mean-squared displacement over time (Eq. 3) for 28 to 76 cells from duplicate platings for each ECM protein concentration (Table I). For HSMC migration, speed follows a normal distribution truncated at zero speed whereas persistence time follows an exponential distribution (DiMilla et al., 1992*b*).

In Fig. 3, *a–c* %-motile cells, mean speed, and mean persistence time are plotted as functions of adsorbed concentration of Fn and CnIV. We found that %-motile cells, defined as the fraction of cells observed to move significantly (see Materials and Methods for a rigorous definition of an immotile cell), depended on the absorbed concentration of Fn and CnIV (Fig. 3 *a*). Maxima in %-motile cells occurred at intermediate concentrations of both ECM proteins and were significant at $p < 0.01$ by an analysis of variance. The peak for Fn, 1.0×10^3 molecules/μm^2, occurred at a surface coverage ~1/10 of the optimum for CnIV, 2.6×10^4 molecules/μm^2. The peak value on CnIV was slightly greater than that on Fn.

Fig. 3 *b* demonstrates that speed also varied with the adsorbed concentration of Fn and CnIV. A maximum mean

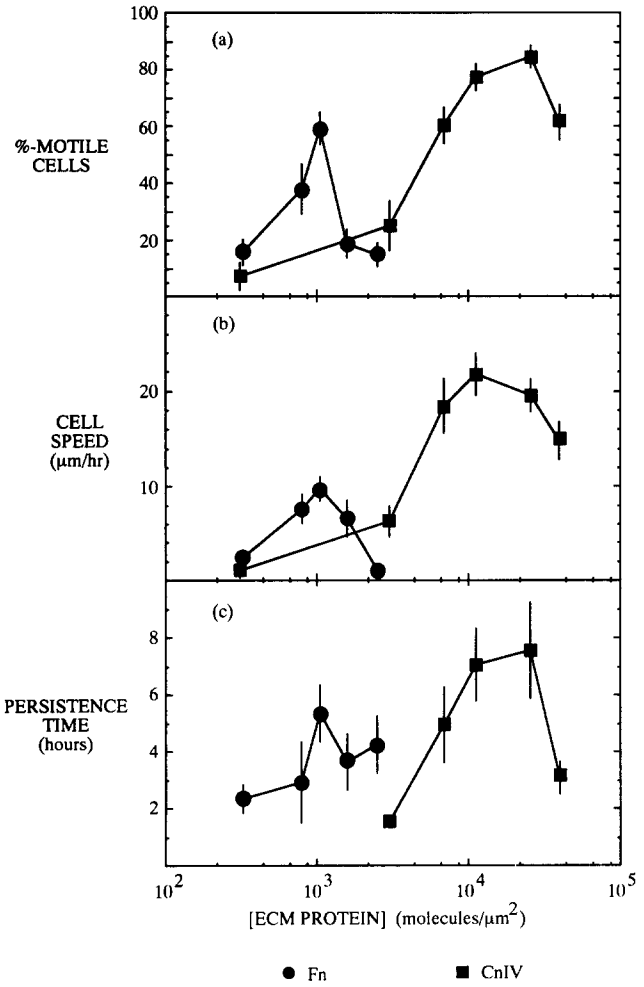

Figure 3. Effect of surface concentrations of adsorbed Fn and CnIV on the motility of HSMCs. Individual cell migration assays, including time-lapse videomicroscopy, image analysis, and analysis with persistent random walk model, were conducted on bacteriological polystyrene dishes coated sequentially with Fn or CnIV and BSA. Protein concentrations adsorbed to dishes were determined from a companion study of protein adsorption as reported in DiMilla et al. (1992*c*), summarized in Table I. All techniques are described in detail in Materials and Methods. The total number of cells and the number of motile cells observed at each protein concentration in duplicate experiments are indicated in Table I. (*a*) %-motile cells, calculated as the fraction of cells observed to translocate (along with SDs) as a function of surface protein concentration. (*b*) Cell speed, *S*, plotted as the mean and SEM for all cells examined as a function of surface protein concentration. (*c*) Means and SEMs for persistence, *P*, based on motile cells as a function of surface protein concentration.

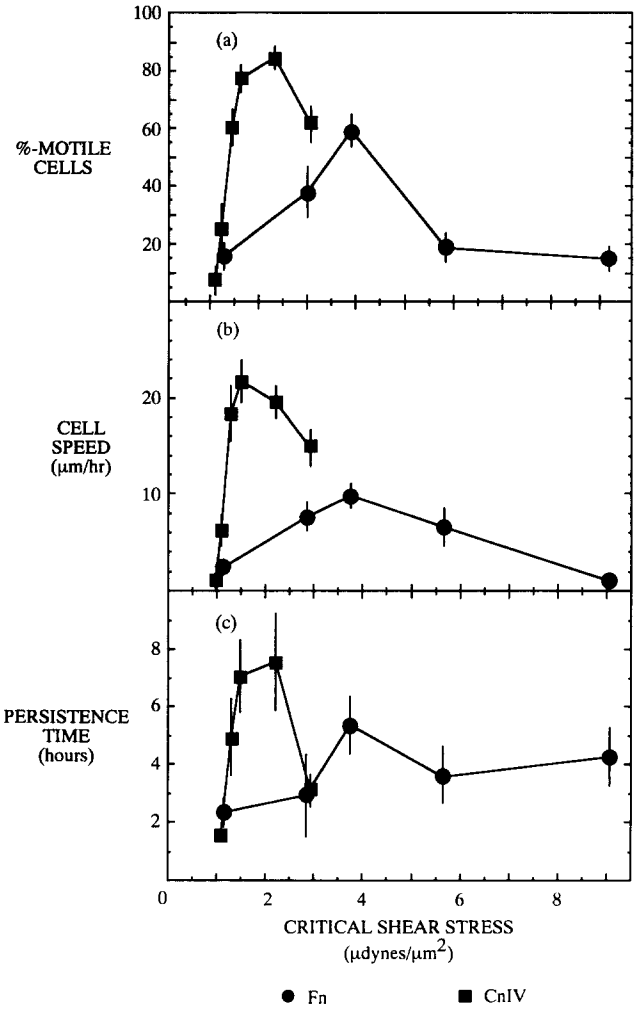

Figure 4. Relationship between strength of initial cell–substratum attachment and %-motile cells, mean speed, and mean persistence time for HSMCs on Fn and CnIV. Data from Fig. 3, *a–c* are plotted against critical shear stress for detachment, s_c (determined from linear least-squares fits of data in Fig. 1), at each surface concentration examined in migration assays.

speed of 10 μm/h occurred on Fn whereas the maximum mean speed on CnIV was about 20 μm/h. From an analysis of variance the maximum in speed for Fn was significant at $p < 0.01$ at 1.0×10^3 molecules/μm², and for CnIV it was significant at $p < 0.05$ between 7.0×10^3 and 2.6×10^4 molecules/μm².

Mean persistence time for motile HSMCs on CnIV varied from 2 to 3 h at relatively low and high concentrations of 3.0×10^3 and 4.0×10^4 molecules/μm², respectively, to a maximum of ~7 h at intermediate concentrations of 7.0×10^3 to 1.1×10^4 molecules/μm² (Fig. 3 *c*). The variation of persistence time on the Fn concentration was less dramatic, although a maximal value was found again at roughly an order of magnitude lower concentration than that for CnIV.

Cell Speed for HSMCs Is Maximal at an Intermediate Attachment Strength for Fn and CnIV

Taken altogether, the data in Figs. 1 and 3 demonstrate that the strength of HSMC–substratum attachment increased with surface concentration of absorbed Fn and CnIV, but that %-motile cells, mean cell movement speed, and mean persistence time attained maximal values at intermediate concentrations of both proteins. However, distinct ranges of surface concentrations for the two proteins were required to achieve these effects; in particular, the absorbed protein concentration for maximum speed on CnIV was approximately ten times greater than the corresponding concentration for Fn. Thus, surface concentration does not satisfactorily correlate cell motility on both proteins. Therefore, we plot these quantities instead as functions of the critical shear stress for detachment for both Fn and CnIV to more directly

assess the relationship between the rate of migration and cell–substratum attachment.

Values for s_c at the concentrations of ECM protein at which cell motility properties were determined (Table I) were calculated from linear least-squares fits of experimental data from the RFDA, and the values of %-motile cells, mean speed, and mean persistence time corresponding to these concentrations were plotted versus s_c (Fig. 4). Motility properties on both Fn and CnIV are captured within a single order of magnitude of the cell–substratum interaction variable instead of being separated by an order of magnitude. Fig. 4 shows directly, for example, that speed is greatest at a similar attachment strength regardless of which ECM protein was chosen as the adhesive ligand, with optimal shear stresses for detachment on the order of a few μdyne/μm^2; more precisely, these optimal values were 3.8 μdynes/μm^2 on Fn and 1.5 dynes/μm^2 on CnIV. Further, a minimum attachment strength corresponding to a detachment shear stress of $\sim$1 μdyne/μm^2 was required for migration on both of these two substrates. Movement behavior on CnIV could not be tested for initial adhesion strengths $> \sim$3 μdynes/μm^2 because such levels could not be produced with this protein and assay.

Discussion

Cell movement over adhesive surfaces is a complex process involving dynamic interactions between cytoskeletal, cell surface, and extracellular components. In this study we have examined the relationship between the adhesive and motile behavior of HSMCs on non-tissue culture surfaces uniformly coated with a range of concentrations of the ECM proteins Fn and CnIV. These cells express on their surface the integrins VLA-5 and VLA-2, which bind Fn and CnIV, respectively (S. Albelda, unpublished observations). We have focused on identifying and measuring quantitative properties, such as the critical fluid shear stress for detachment and the individual cell movement speed and persistence time, which intrinsically characterize the effect of variations in substratum properties on cell adhesion and motility. Our major findings are: (*a*) the critical shear stress required to detach adherent cells, a measure of the strength of initial cell–substratum attachment, increases linearly with the surface concentration of both Fn and CnIV; (*b*) on a per absorbed protein molecule basis, the initial attachment strength is much greater on Fn than on CnIV; (*c*) the fraction of motile cells and mean migration speed demonstrate maxima at intermediate concentrations of Fn and CnIV, with the optimal CnIV concentration ten times greater than the optimal Fn concentration; and, (*d*) migration properties on Fn and CnIV are more satisfactorily correlated by the initial strength of cell–substratum attachment than by absorbed protein concentration, the optimal attachment strength for maximal migration speed being of similar magnitude for both of these ECM proteins.

We applied a radial-flow detachment assay (Cozens-Roberts et al., 1990; DiMilla et al., 1992*a*) to measure quantitatively the attachment of HSMCs after incubation for 30 min to adsorbed Fn and CnIV. Because adherent cells in the RFDA are exposed to a better-defined and continuous range of detachment forces than cells in conventional washing assays, the measured adhesive response to increasing concentration of ECM protein does not saturate even at high concentrations of ECM protein. Rather, increasing the concentration of Fn or CnIV increases the overall rate for formation of bonds, allowing cells to resist progressively greater forces of detachment (Bell, 1978). Saturation in the fraction

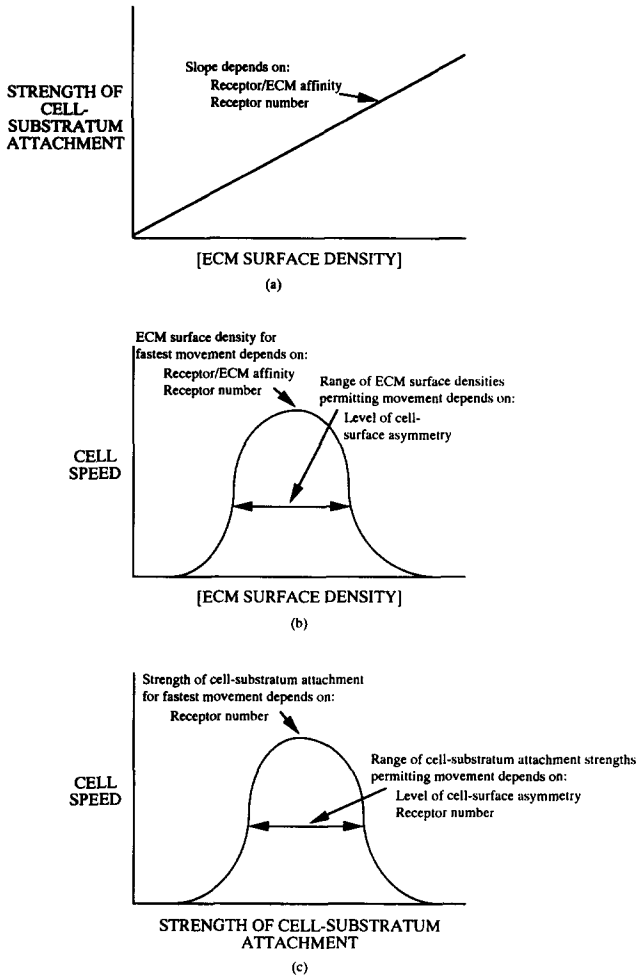

Figure 5. Schematic of the relationship between surface concentration of ECM protein, strength of cell–substratum attachment, and cell speed, based on experimental observations presented in this study and predictions of theoretical models for cell–substratum adhesion (Cozens-Roberts et al., 1990) and cell migration over adhesive surfaces (DiMilla et al., 1991). (*a*) Strength of cell–substratum attachment, measurable as the critical force necessary for detachment (or s_c), increases linearly with surface concentration of ECM protein (compare with Fig. 1). The slope of this line is predicted to increase with increasing adhesion-receptor/ECM protein affinity or receptor number. (*b*) An optimal surface concentration of ECM protein exists for cell movement speed (compare to Fig. 3*b*). The specific surface concentration of ECM protein for maximum speed is predicted to increase with decreasing receptor number and adhesion-receptor/ECM protein affinity. The range of surface concentration of ECM protein allowing movement is predicted to depend on the magnitude of the asymmetry in the cell-substratum interaction between front and rear of the cell. (*c*) An optimal strength of cell-substratum attachment exists for cell movement speed (compare with Fig. 4). The strength of attachment for maximum speed is predicted to increase with decreasing receptor number. Both increasing cell–surface asymmetry and receptor number increase the range of attachment strength allowing significant movement.

of cells adhered is frequently observed in conventional washing assays because only a limited force of detachment is applied, and cells cannot be detached from surfaces in which the adhesive strength is greater than this arbitrary force. Further, the linear relationships we observed between the critical detachment shear stress, s_c, and the surface concentration of CnIV and Fn are consistent with a theoretical model for receptor-mediated adhesion (Cozens-Roberts et al., 1990) which predicts how s_c varies with key cell and substratum biochemical and biophysical properties (Fig. 5 *a*). This model predicts that the slope of the relationship between strength of initial cell–substratum attachment and the surface concentration of ECM protein increases with both increasing adhesion-receptor number and affinity between adhesion receptor and ECM protein. Thus, the steeper slope observed on Fn-coated compared to CnIV-coated surfaces may be due to a greater number of cell surface receptors for Fn than for CnIV or a stronger receptor affinity for Fn than for CnIV.

Migration over adhesive surfaces is a dynamic phenomenon involving the formation and breakage of attachments with an underlying substratum (Regen and Horwitz, 1992). Both short-term interactions—such as binding between individual adhesion receptors and substratum-bound ligand—and longer time-scale events (e.g., clustering of adhesion receptors into focal contacts [Burridge et al., 1988] and the formation of stress fibers [Dejana et al., 1987]) may be relevant to movement occurring over periods of many hours. The relative contributions of these different time-scale adhesive interactions to cell locomotion presently are poorly understood. In this study we have focused on initial attachment strength in order to characterize the short time-scale effects. Incubating cells with surfaces for 30 min before initiation of detachment allows stable attachment while limiting cell spreading and cytoskeletal and cell surface reorganization. For tissue cells exhibiting typical locomotion rates on the order of 10–20 μm/h, attachments must be dynamic on this time scale of a few hours or less. Because our data indicate that a similar intermediate strength of these short time-scale attachment events correlates maximal rates of migration on both ECM proteins, we suggest that variations in the strength of individual adhesive bonds are relevant to movement. Quantitatively distinguishing transient receptor/ligand-mediated events from adhesion governed by organized receptor-cytoskeletal interactions, which currently can be addressed only by qualitative examination of cell morphology and the structure of molecular linkages, is a critical consideration for future experiments and requires the development of assays in which the comparative contributions of different modes of detachment can be assessed.

By describing the movement of individual HSMCs as a persistent random walk (DiMilla et al., 1992*b*), we could distinguish variations in speed from changes in the rate of turning in response to increasing concentrations of ECM protein. Fig. 3 shows that speed has a biphasic dependence on absorbed protein concentration, although the concentration at which significant migration occurs is greater by an order of magnitude for CnIV than for Fn. Following Fig. 1, a plausible explanation is that cell–substratum attachment is much stronger on a molecular basis for Fn than for CnIV. Fig. 1 also offers one possible explanation for why the decreasing portion of the biphasic speed versus protein concentration curve is less complete for CnIV than for Fn, because sufficiently great levels of attachment strength were not achieved using these concentrations of CnIV. This limitation also may at least partially account for other experimental findings in which migration speed shows a monophasic dependence on protein concentration for some ligands along with a biphasic dependence for others.

The existence of distinctly separate optimal concentrations of Fn and CnIV for maximal HSMC speed may be related to the observations of Duband et al. (1991) for the effect of variations in adsorbed ligand concentration and affinity on the motility of neural crest cells on anti-integrin antibodies. Their data show an increasing extent of migration as the concentration of low-affinity ligands increases, but a decreasing extent of migration as the concentration of high-affinity ligands increases (with the ligands present over the same range of concentrations). Our results in Fig. 3 *b* are consistent with the results of Duband et al. (1991) and we have additionally extended the range of ligand concentrations. We have not provided direct measurement of Fn or CnIV binding affinity to HSMC receptors in this study, but have instead focused on cell–substratum attachment strength as a functional reflection of affinity. Both of these studies are consistent with the biphasic relationship between speed and concentration of ECM protein predicted by a recent theoretical model for the effect of receptor-mediated adhesion on cell movement speed over adhesive surfaces (DiMilla et al., 1991). This model predicts that the surface concentration of ECM protein for maximum speed increases with decreasing adhesion-receptor number and adhesion-receptor/ECM-protein affinity (Fig. 5 *b*).

Indeed, the model by DiMilla et al. (1991) offers a quantitative explanation for the observation (Fig. 3) that migration occurs over ECM absorbed protein concentration ranges separated by an order of magnitude, because it considers cell–substratum adhesion strength—rather than ligand concentration itself—as a primary variable governing migration speed (Fig. 5 *c*). When migration properties are plotted directly as functions of attachment strength (Fig. 4) it is evident that this quantity correlates behavior on the two different ECM proteins much better than does protein concentration alone. The intermediate, optimal value of the attachment strength yielding maximal movement is predicted by the model to vary with receptor number, which may differ for Fn and CnIV in the case of HSMCs.

Another important prediction of this model is that the range of concentrations of ECM protein permitting migration depends on the level of polarization in the strength or number of adhesion–receptor/ECM–protein interactions between lamellipod and uropod. At least three underlying mechanisms are possible for such a front-to-back asymmetry in cell–substratum interactions: a spatial distribution of receptor number due to preferential trafficking of receptors to the leading edge (Bretscher, 1992), a spatial variation in receptor/ECM protein affinity between lamellipod and uropod (Dustin and Springer, 1989), and/or a spatial variation in receptor/cytoskeleton linkage. The magnitude of the maximal speed itself is predicted by this model to be affected by a number of factors, including the ability of adhesion receptors to interact with the cytoskeleton for transmission of intracellular motile force and the level of this force itself. Hence, the greater value of maximal speed exhibited in this

study by HSMCs on CnIV compared to that on Fn may reflect an underlying difference in cytoskeleton interactions or signaling by the corresponding integrins. Thus, it should be clear that although cell-substratum adhesiveness may be a central variable in governing migration properties, there are other important variables—such as motile force generation and receptor-cytoskeleton linkage—which can depend on adhesion receptor-ligand interactions and consequent signals. For example, Calof and Lander (1991) have shown that laminin affects neuronal cell migration by means not directly related to adhesiveness.

Finally, data on the variation of persistence time, characterizing cell directional turning frequency, are rare. Fig. 3 *c* demonstrates that this aspect of migration may also be related to cell-substratum adhesion properties, although the model by DiMilla et al. (1991) does not address this issue. Kinetic properties of receptor-ligand interactions may influence turning frequency, as predicted by Dickinson and Tranquillo (1993).

The authors thank Mildred Daise for help with cell culture, Ann O'Hara for assistance with analysis of HSMC motility, and Stuart Williams of Thomas Jefferson University, and Eliott Levine of the Wistar Institute for providing CnIV and HSMCs, respectively. Helpful discussions with Jon Edelman, Clayton Buck, and Rick Horwitz are also appreciated.

This work was supported by a grant from the Whitaker Foundation to S. M. Albelda and National Institutes of Health Grant GM-41476 to D. A. Lauffenburger.

Received for publication 2 October 1992 and in revised form 10 April 1993.

References

Akiyama, S. K., and K. M. Yamada. 1985. The interaction of plasma fibronectin with fibroblastic cells in suspension. *J. Biol. Chem.* 260:4492–4500.

Albelda, S. M., and C. A. Buck. 1990. Integrins and other cell adhesion molecules. *FASEB (Fed. Am. Soc. Exp. Biol.) J.* 4:2868–2880.

Basson, C. T., W. J. Knowles, L. Bell, S. M. Albelda, L. A. Liotta, and J. A. Madri. 1990. Spatiotemporal segregation of bovine aortic endothelial-cell integrin and non-integrin extracellular matrix-binding proteins during adhesion events. *J. Cell Biol.* 110:789–801.

Bauer, J. S., C. L. Schreiner, F. G. Giancotti, E. Ruoslahti, and R. L. Juliano. 1992. Motility of fibronectin receptor-deficient cells on fibronectin and vitronectin: collaborative interactions among integrins. *J. Cell Biol.* 116: 477–487.

Bell, G. I. 1978. Models for the specific adhesion of cells to cells. *Science (Wash. DC).* 200:618–627.

Bretscher, M. S. 1992. Circulating integrins: $\alpha_5\beta_1$, $\alpha_6\beta_4$ and Mac-1, but not $\alpha_3\beta_1$, $\alpha_4\beta_1$ or LFA-1. *EMBO (Eur. Mol. Biol. Organ.) J.* 11:405–410.

Burridge, K., K. Faith, T. Kelly, G. Nuckolls, and C. Turner. 1988. Focal adhesions: transmembrane junctions between the extracellular matrix and the cytoskeleton. *Annu. Rev. Cell Biol.* 4:487–525.

Calof, A. L., and A. D. Lander. 1991. Relationship between neuronal migration and cell-substratum adhesion: laminin and merosin promote olfactory neuronal migration but are anti-adhesive. *J. Cell Biol.* 115:779–794.

Clyman, R. I., D. C. Turner, and R. H. Kramer. 1990. An α_1/β_1-like integrin receptor on rat aortic smooth muscle cells mediates adhesion to laminin and collagen types I and IV. *Arteriosclerosis.* 10:402–409.

Cozens-Roberts, C., D. A. Lauffenburger, and J. A. Quinn. 1990. Receptor-mediated adhesion phenomena: Model studies with the radial-flow detachment assay. *Biophys. J.* 58:107–125.

Dejana, E., S. Colella, L. R. Languino, G. Balconi, G. C. Corbascio, and P. C. Marchiso. 1987. Fibrinogen induces adhesion, spreading, and microfilament organization of human endothelial cells. *J. Cell Biol.* 104: 1403–1411.

Devreotes, P. N., and S. H. Zigmond. 1988. Chemotaxis in eukaryotic cells: a focus on leukocytes and *Dictyostelium. Ann. Rev. Cell Biol.*; 4:649–686.

Dickinson, R. B., and R. T. Tranquillo. 1993. A stochastic model for cell random motility and haptotaxis based on adhesion receptor binding fluctuations. *J. Math. Biol.* In press.

DiMilla, P. A., K. Barbee, and D. A. Lauffenburger. 1991. Mathematical model for the effects of adhesion and mechanics on cell migration speed. *Biophys. J.* 60:15–37.

DiMilla, P. A., J. A. Stone, S. M. Albelda, D. A. Lauffenburger, and J. A. Quinn. 1992*a*. Measurement of cell adhesion and migration on protein-coated surfaces. *In* Tissue-Inducing Biomaterials. L. G. Cima and E. S. Ron, editors. Mater. Res. Soc. Proc. Pittsburgh, PA. Vol. 252, 205–212.

DiMilla, P. A., S. M. Albelda, D. A. Lauffenburger, and J. A. Quinn. 1992*b*. Measurement of individual cell migration parameters for human tissue cells. *AIChE J.* 37:1092–1104.

DiMilla, P. A., S. M. Albelda, and J. A. Quinn. 1992*c*. Adsorption and elution of extracellular matrix proteins on non-tissue culture polystyrene petri dishes. *J. Colloid. Interface Sci.* 153:212–225.

Duband, J.-L., S. Dufour, S. S. Yamada, K. M. Yamada, and J. P. Thiery. 1991. Neural crest cell locomotion induced by antibodies to β_1 integrins: a tool for studying the roles of substratum molecular avidity and density in migration. *J. Cell Sci.* 98:517–532.

Dunn, G. A. 1983. Characterizing a kinesis response: time-averaged measures of cell speed and directional persistence. *Agents Actions Suppl.* 12:14–33.

Dustin, M. L., and T. A. Springer. 1989. T-cell receptor cross-linking transiently stimulates adhesiveness through LFA-1. *Nature (Lond.).* 341:619–624.

Gail, M. H., and C. W. Boone. 1970. The locomotion of mouse fibroblasts in tissue culture. *Biophys. J.* 10:980–993.

Goodman, S. L., G. Risse, and K. von der Mark. 1989. The E8 subfragment of laminin promotes locomotion of myoblasts over extracellular matrix. *J. Cell Biol.* 109:799–809.

Heath, J. P., and B. F. Holifield. 1991. Cell locomotion: new research tests old ideas on membrane and cytoskeletal flow. *Cell Motil. Cytoskel.* 18: 245–257.

Hemler, M. E. 1990. VLA proteins in the integrin family: structures, functions, and their roles on leukocytes. *Annu. Rev. Immunol.* 8:365–400.

Horwitz, A. F., K. Duggan, C. Buck, M. C. Beckerle, and K. Burridge. 1986. Interaction of plasma membrane fibronectin receptor with talin: transmembrane linkage. *Nature (Lond.).* 320:531–532.

Hynes, R. O. 1987. Integrins: a family of cell surface receptors. *Cell.* 48: 549–554.

Lackie, J. M. 1986. Cell Movement and Cell Behavior. Allen and Unwin, London.

Mendenhall, W., and T. Sincich. 1992. Statistics for Engineering and the Sciences. Dellen Publishing Co., San Francisco, CA.

Regen, C. M., and A. F. Horwitz. 1992. Dynamics of β_1 integrin-mediated adhesive contacts in motile fibroblasts. *J. Cell Biol.* 119:1347–1359.

Ross, R. 1986. The pathogenesis of atherosclerosis—an update. *New Eng. J. Med.* 314:488–500.

Singer, S., and A. Kupfer. 1986. The directed migration of eukaryotic cells. *Annu. Rev. Cell Biol.* 2:337–365.

Stein, W. D., and F. Bronner. 1989. Cell Shape: Determinants, Regulation, and Regulatory Role. Academic Press, San Diego, CA.

Stokes, C. L., D. A. Lauffenburger, and S. K. Williams. 1991. Migration of individual microvessel endothelial cells: stochastic model and parameter measurement. *J. Cell Sci.* 99:419–430.

Straus, A. H., W. G. Carter, E. A. Wayner, and S.-I. Hakomori. 1989. Mechanism of fibronectin-mediated cell migration: dependence or independence of cell migration susceptibility on RGDS-directed receptor (integrin). *Exp. Cell Res.* 183:126–139.

Tan, E. M. L., G. R. Dodge, T. Sorger, I. Kovalszky, G. A. Unger, L. Yang, E. M. Levine, and R. V. Iozzo. 1991. Modulation of extracellular matrix gene expression by heparin and endothelial cell growth factor in human smooth muscle cells. *Lab. Invest.* 64:474–482.

Trinkaus, J. P. 1984. Cells Into Organs: The Forces that Shape the Embryo. Prentice-Hall, Inc., Englewood Cliffs, NJ.

Yamada, K. M. 1989. Fibronectin domains and receptors. *In* Fibronectin. D. F. Mosher, editor. Academic Press, Inc., New York. 47–121.